

doi.org/10.15407/ujpe68.7.488

O.R. BARAN

Institute for Condensed Matter Physics, Nat. Acad. of Sci. of Ukraine
(1, Svientitskii Str., Lviv 79011, Ukraine; e-mail: ost@ph.icmp.lviv.ua)**MAGNETOCALORIC EFFECT
IN THE ONE-DIMENSIONAL SPIN- $\frac{1}{2}$ XX MODEL
WITH TWO PERIODICALLY VARYING g -FACTORS**

The influence of a non-uniformity of the g -factors with period two on the magnetocaloric effect in the spin- $\frac{1}{2}$ XX chain in the transverse field has been studied. By means of the Jordan–Wigner transformation, the problem is reduced to the Hamiltonian of noninteracting spinless fermions and solved exactly. The variation of isentropes and the field dependences of the magnetic Grüneisen ratio with a change in the ratio g_2/g_1 are analyzed. Main attention is paid to the low-temperature region. Distinctions among the magnetocaloric effect manifestations in the cases where the g -factors have different or identical signs, or if either of g -factors equals zero, are demonstrated.

Keywords: one-dimensional quantum spin models, g -factor, Jordan–Wigner fermionization, magnetocaloric effect, quantum phase transition.

1. Introduction**1.1. One-dimensional systems
with periodically varying g -factors**

Among the magnetic materials, there are a number of compounds that can be adequately described on the basis of spin chains with periodically varying g -factors. In particular, the magnetic properties of the molecular magnet $[\{\text{Co}^{\text{II}}(\Delta)\text{Co}^{\text{II}}(\Lambda)\}(\text{ox})_2(\text{phen})_2]_n$ can be explained with the help of the Ising chain with two different g -factors at neighboring sites ($g_1 = 2.5$, $g_2 = 2.1$) and by two different exchange interactions [1]. In work [2], the Heisenberg and Ising spin-1 $g_1 - g_2$ chains with antiferromagnetic interactions were applied to model the one-dimensional (1D)

two-sublattice system $\text{Ni}_2(\text{EDTA})(\text{H}_2\text{O})_4 \cdot 2\text{H}_2\text{O}$, and good agreement between the theory and the experiment was obtained for $g_2/g_1 = 1.1$. One-dimensional complex oxide $\text{Sr}_3\text{CuIrO}_6$, which contains both $3d$ (Cu^{2+}) and $5d$ (Ir^{4+}) magnetic ions, can be described using the spin- $\frac{1}{2}$ Heisenberg ferromagnetic model with easy-axis magnetic anisotropy ($\gamma = J^z/J^x = J^z/J^y \approx 2.55$) and a periodically varying g -factor with period two (the copper ions have the spin with $g \approx 2$, and the iridium ions the isospin with $g \approx -3$) [3, 4]. Note that the g -factors at neighboring sites are of identical signs in the first two substances mentioned above and have different signs in the third one.

It is also pertinent to mention the compounds that are described by somewhat more complicated one-dimensional spin models. For instance, the heterotrimeric coordination polymer



can be approximately considered (see work [5]) as a spin- $\frac{1}{2}$ Ising chain whose sites are alternately occu-

Citation: Baran O.R. Magnetocaloric effect in the one-dimensional spin-1/2 XX model with two periodically varying g -factors. *Ukr. J. Phys.* **68**, No. 7, 488 (2023). <https://doi.org/10.15407/ujpe68.7.488>.

Цитування: Баран О.Р. Магнетокалоричний ефект у спин-1/2 одновимірній XX моделі з двома регулярнозмінними g -факторами. *Укр. фіз. журн.* **68**, № 7, 490 (2023).

pied by iron Fe^{3+} and manganese Mn^{2+} ions with additional copper Cu^{2+} ions; the latter are “side-connected” to manganese ions with the anisotropic Heisenberg (XXZ) exchange interaction. Values of g -factors for Fe^{3+} , Cu^{2+} , and Mn^{2+} were put equal 2.4, 2.2, and 10, respectively. The value $g_{\text{Mn}} = 10$ for the manganese ion was associated with the fact that, in the cited work, all ions were assigned the spin $s = \frac{1}{2}$ (to simplify the problem), whereas it should be $s = 5/2$ for Mn^{2+} .

Another example is the infinite polymer chain $[\text{DyCuMoCu}]_{\infty}$, in which there is, so to speak, a next-neighbor interaction between the dysprosium and the molybdenum [6]. The unit cell of this compound contains four magnetic ions with three different g -factor values. Moreover, the dysprosium ions Dy^{3+} are described by Ising spins, and the copper Cu^{2+} and molybdenum Mo^{5+} ions by Heisenberg spins. Since the Ising spins are decorated by $[\text{CuMoCu}]$ trimeric Heisenberg units, this problem can be solved exactly.

In order to explain certain experimental results obtained for the coordination compound copper benzoate, in works [7, 8], there was considered a spin model with the sign-alternating (for neighboring sites) Dzyaloshinsky–Moriya interaction and a g -tensor whose certain elements are also sign-alternating. Those sign alternations bring about an effective model, namely, the Heisenberg model with a sign-alternating magnetic field along the x -axis and a uniform field along the z -axis (which is equivalent to a periodically varying g -factor). A similar model was also used in work [9] to model the spin- $\frac{1}{2}$ antiferromagnetic chain $\text{CuCl}_2 \cdot 2[(\text{CD}_3)_2\text{SO}]$.

1.2. Jordan–Wigner transformation

While researching various one-, two-, and three-dimensional spin systems, widely applied are approaches and approximations in which various variants of the Jordan–Wigner fermionization are used (see review [10]). The advantage of such methods is that strongly correlated spin states can be compactly described in terms of fermion excitations. For the first time, the one-dimensional Jordan–Wigner transformation was implemented more than half a century ago in paper [11] for the spin- $\frac{1}{2}$ XY chain. As a result of the fermionization, the problem was reduced to the Hamiltonian of non-interacting spinless fermions and solved exactly.

Later, on the basis of such a one-dimensional fermionization, both exact and approximate results were obtained for the thermodynamic and dynamic characteristics of a number of one-dimensional models. For example, in works [12, 13], the problem of one-dimensional spin- $\frac{1}{2}$ XX chain in a transverse field with two different g -factors (g_1 and g_2) at neighboring sites was solved exactly. In work [12], besides the g -factors, exchange interactions were also assumed to be periodic with the same period (two). The cited authors confined the consideration to thermodynamic characteristics in the case where g_1 and g_2 have the same sign.

In paper [13], however, the research was carried out for both the $g_1 g_2 > 0$ and $g_1 g_2 \leq 0$ cases. Main attention was focused on the analysis of dynamic characteristics, namely, the transverse and longitudinal absorption intensities [they are observed in electron spin resonance (ESR) experiments], and the dynamic structure factors (they can be studied in neutron magnetic scattering experiments). Expressions for all studied quantities were obtained analytically except for the longitudinal structural factor, which was calculated using the method developed in works [14, 15].

In paper [16], a one-dimensional spin- $\frac{1}{2}$ anisotropic XY model in a transverse field with periodically varying g -factors and periodically varying exchange interactions with the same (for both microscopic parameters) but arbitrary period was considered. Accurate results were obtained for some thermodynamic characteristics, as well as for the zz pair dynamic correlation function and the zz dynamic susceptibility.

Among the set of works, where rigorous results were obtained due to the implementation of the one-dimensional Jordan–Wigner transformation, there can be mentioned, for example, those, where the Hamiltonian contains not only two-spin interactions but also three-spin ones (see, e.g., works [17–24]). In particular, papers [23, 24] were devoted to the study of one-dimensional magnetoelectrics, where the coupling of localized spins (i.e., magnetic moments) with the electric polarization of the bond connecting those spins is described by the Katsura–Nagaosa–Balatsky mechanism [25]. Menchyshyn *et al.* [23] showed that the additional account for three-spin interactions can result in a non-trivial magnetoelectric effect (the induction of the electric polarization by a magnetic field at the zero electric field and vice versa), which is not realized in 1D magnetoelectrics with only pair

exchanges [26–28]. In work [24], three-spin interactions ($XZY - YZX$ and $XZX + YZY$) arose, so to speak, naturally when considering the stationary energy flow on the basis of the Lagrange multiplier method (see works [17, 29]) in the one-dimensional spin- $\frac{1}{2}$ isotropic XY model of the magnetoelectric with only two-spin interactions. It is also worth singling out work [20], where a rigorous result was obtained for the XX model not only with three-spin interactions ($XZY - YZX$), but also with a uniform long-range pair interaction between the spin z -components.

Not all 1D spin models in the framework of the Jordan–Wigner transformation provide exact solutions. For example, in work [30], to study an anisotropic XY linear chain with uniform long-range Ising interaction in a magnetic field directed along the z -axis, a mean-field-type approximation was implemented for the direct interaction between fermions, similarly to what was done in the case of one-dimensional anisotropic XXZ and XYZ models in a transverse field [31, 32]. A certain approximation procedure after the fermionization has also been performed for the spin- $\frac{1}{2}$ diamond XX chain. In particular, the phase factors were neglected in work [33], and the Hartree–Fock approximation was used in work [34].

If talking about systems with dimensionalities higher than one, then, for example, in work [35], one of the generalizations of the one-dimensional Jordan–Wigner transformation was realized in the case of the spin- $\frac{1}{2}$ Heisenberg model on a square lattice (see also works [36, 37] and review [10]). The transformed Hamiltonian corresponds to interacting spinless fermions that jump between neighboring sites in a fictitious gauge magnetic field that was generated in this approach. Using an approximation of the mean-field type for both the direct interaction between fermions and the phase multipliers corresponding to the gauge field, the problem was reduced to a free Fermi gas, and the properties of the ground state were examined [35]. Later, this method was adapted to study other systems, in particular, the anisotropic and isotropic XY models on a rectangular lattice [38–40], and the frustrated Heisenberg model with interactions between nearest and next-nearest neighbors [41, 42]. It should be noted that the flow of the strength vector of the fictitious magnetic field was considered in the cited works to be identical for all rectangular elementary plaques. At the same time,

for example, in work [43] (see also work [44]), it was considered to depend on the magnetization of only one site (e.g., the upper left one) “adjacent” to this plaque.

1.3. Formulation of the problem. Magnetocaloric effect

This work continues the study of the properties of the one-dimensional spin- $\frac{1}{2}$ $g_1 - g_2$ XX model in a transverse field, which was started in work [13]. As was already mentioned above, this model in the framework of the Jordan–Wigner transformation has exact solutions. The results obtained for such a simplified problem may be useful for explaining certain properties of systems described by a Heisenberg chain with different g -factors at neighboring sites. For example, it was found in work [13] that logarithmic singularities in the magnetization curve and the static susceptibility at the zero field (the latter is a result of the periodicity of the g -factor in real magnets) are a consequence of an unexpected effect, when the sublattice with a smaller g -factor begins to become ordered in the direction opposite to the field due to the quantum-mechanical interaction between the spins. Eventually, the energy of those magnetic ions in the field prevails, and all magnetic moments become oriented along the magnetic field.

In the same paper [13], some dynamic characteristics were also calculated, which made it possible to reveal the non-uniformity of g -factors in experiments on the magnetic neutron scattering and electron spin resonance. In particular, the model of uniform g -factors ($g_1 = g_2$) did not demonstrate any response in the Voigt ESR configuration. In the case of different g_1 and g_2 , the corresponding absorption intensity was found to be able to differ from zero, and, at sufficiently high frequencies, it had a van Hove singularity. In the Faraday ESR configuration, the absorption spectrum with a deviation from the uniform case showed a resonance line doubling.

Based on the results obtained in work [13], in this work, the magnetocaloric effect (MCE) will be studied in both the $g_1 g_2 > 0$ and $g_1 g_2 \leq 0$ cases. In particular, such important characteristics of this effect as isentropes (see, e.g., works [27, 45–47]) and the intensity of adiabatic cooling (see, e.g., works [22, 46, 47]) will be calculated and analyzed. It will be shown how the above-mentioned quantities change with a deviation

tion from the uniform case, and how they are different in the $g_1 g_2 > 0$, $g_2 = 0$, and $g_1 g_2 < 0$ cases.

It should be said that the MCE, namely, a change in the magnetic material temperature, when the external magnetic field changes, has been known since the end of the 19th century [48]. A successful MCE-based adiabatic demagnetization experiment was performed for the first time in 1993 [49], and methods similar by principles are now standard ones when obtaining low and ultralow temperatures (see works [50–52]). Nowadays, the MCE also draws considerable attention in connection with the possibility of creating cooling devices that could operate, in particular, at room temperatures [53, 54]. Another important property of the magnetocaloric effect is its, so to speak, response [55, 56] to the presence of a quantum phase transition (the proximity to the quantum critical point manifests itself in the MCE in the low-temperature region).

In view of the problem under consideration, it is also pertinent to mention that there are a number of papers, where the magnetocaloric effect in spin systems (both one- [22, 27, 45, 46, 57–62], and two-dimensional ones [63–65]) was studied on the basis of rigorous results obtained in the framework of various approaches. In particular, the MCE in the spin- $\frac{1}{2}$ XX 1D model with three-spin interactions of the types $XZX + YZY$ and $XZY - YZX$ was considered in work [22] using the one-dimensional Jordan–Wigner transformation. In papers [45] and [27], the isentropes for the spin- $(\frac{1}{2}, s)$ Ising–Heisenberg rhombic chain were analyzed using the decoration-iterative transformation, and those for the spin- $\frac{1}{2}$ XX magnetoelectric chain with zigzag geometry were studied in the framework of the fermionization method. In work [46], by applying the transfer matrix technique to the spin- $\frac{1}{2}$ XXZ one-dimensional model, and, in work [62] for the spin- $(\frac{1}{2}, 1)$ decorated Ising–Heisenberg sawtooth ladder, the Grüneisen magnetic parameters, besides the isentropes, were also calculated to describe the MCE.

2. Thermodynamic Parameters of Quantum Spin Chains with Periodically Varying g -Factors

Consider a spin- $\frac{1}{2}$ XX chain in a transverse (oriented along the z -axis) magnetic field in the case where the g -factor is a periodically varying function with a pe-

riod of 2. The model Hamiltonian looks like

$$H = \sum_{l=1}^{\frac{N}{2}} \left[-g_1 h s_{2l-1}^z - g_2 h s_{2l}^z + J (s_{2l-1}^x s_{2l}^x + s_{2l-1}^y s_{2l}^y + s_{2l}^x s_{2l+1}^x + s_{2l}^y s_{2l+1}^y) \right]. \quad (1)$$

Here, N is the number of spins in the chain, J the exchange interaction parameter, and h the external magnetic field ($h = \mu_B B$, where $\mu_B \approx 0.67171 \frac{\text{K}}{\text{T}}$ is the Bohr magneton); the dimensions of the fields h and B are kelvin and tesla, respectively. In what follows and without loss of generality, periodic boundary conditions are adopted, and N is assumed an even number.

In the framework of the one-dimensional Jordan–Wigner transformation [11], the problem is reduced to the Hamiltonian of non-interacting spinless fermions. In the momentum space, we have [13]

$$H = \sum_{-\pi \leq \kappa < \pi} \Lambda_\kappa \left(\alpha_\kappa^\dagger \alpha_\kappa - \frac{1}{2} \right), \quad (2)$$

where

$$\Lambda_\kappa = -g_+ h + \text{sgn}(J \cos \kappa) \sqrt{J^2 \cos^2 \kappa + g_-^2 h^2},$$

$$g_\pm = \frac{g_1 \pm g_2}{2}.$$

α_κ^\dagger and α_κ are the creation and annihilation, respectively, operators for a fermion with the quasimomentum $\kappa = 2\pi l/N$ ($l = -N/2, \dots, N/2 - 1$), and Λ_κ is the spectrum of elementary excitations. As was mentioned above, the thermodynamic and transverse dynamic characteristics for problem (2) can be obtained analytically, whereas numerical methods have to be used when calculating the longitudinal dynamic properties (see work [13]).

From the viewpoint of the research carried out in this work, it is important to recall that if $g_1 g_2 > 0$, and if the magnetic field h varies, phase transitions in the ground state from the gapless spin liquid phase into the phase with saturated magnetization occur at $h = h_s$, where $h_s = \pm |J|/\sqrt{g_1 g_2}$ are saturation fields [12, 13]. But if $g_1 g_2 \leq 0$, and the temperature equals zero, the system does not undergo any quantum phase transition with a change in h [13] and remains in a phase, where the Fermi level is located in the forbidden band between two spectral branches and $\langle s_1^z \rangle = -\langle s_2^z \rangle$, where $\langle s_1^z \rangle$ and $\langle s_2^z \rangle$ are the average

values of the spin z -component in two sublattices. It should be noted that the magnetization in the problem with the periodically varying factors g_1 and g_2 obviously equals $m = \frac{1}{2}(g_1 \langle s_1^z \rangle + g_2 \langle s_2^z \rangle)$.

In the thermodynamic limit, on the basis of Eq. (2), it is easy to obtain the free energy per particle [13],

$$\begin{aligned} f(T, h) &= -T \ln \text{Tr} e^{-H/T} = \\ &= -\frac{T}{2\pi} \int_{-\pi}^{\pi} d\kappa \ln \left(2 \cosh \frac{\Lambda_\kappa}{2T} \right) \end{aligned} \quad (3)$$

here, we put $k_B = 1$. In turn, on the basis of Eq. (3), we can obtain other thermodynamic quantities, in particular, the magnetization m , the entropy S , and the heat capacity c (all per particle):

$$\begin{aligned} m(T, h) &= -\frac{\partial f(T, h)}{\partial h} = \frac{1}{4\pi} \int_{-\pi}^{\pi} d\kappa \tanh \left(\frac{\Lambda_\kappa}{2T} \right) \times \\ &\times \left[\frac{\text{sgn}(J \cos \kappa) g_-^2 h}{\sqrt{J^2 \cos^2 \kappa + g_-^2 h^2}} - g_+ \right], \end{aligned} \quad (4)$$

$$\begin{aligned} S &= -\frac{\partial f(T, h)}{\partial T} = \\ &= \frac{1}{2\pi} \int_{-\pi}^{\pi} d\kappa \left[\ln \left(2 \cosh \frac{\Lambda_\kappa}{2T} \right) - \frac{\Lambda_\kappa}{2T} \tanh \frac{\Lambda_\kappa}{2T} \right], \end{aligned} \quad (5)$$

$$\begin{aligned} c(T, h) &= T \frac{\partial S(T, h)}{\partial T} = \\ &= \frac{1}{8\pi T^2} \int_{-\pi}^{\pi} d\kappa \left[\Lambda_\kappa / \cosh \frac{\Lambda_\kappa}{2T} \right]^2. \end{aligned} \quad (6)$$

The expression for the partial derivative $\frac{\partial m(T, h)}{\partial T}$ looks like

$$\begin{aligned} \frac{\partial m(T, h)}{\partial T} &= -\frac{1}{8\pi T^2} \int_{-\pi}^{\pi} d\kappa \Lambda_\kappa \cosh^{-2} \left(\frac{\Lambda_\kappa}{2T} \right) \times \\ &\times \left[\frac{\text{sgn}(J \cos \kappa) g_-^2 h}{\sqrt{J^2 \cos^2 \kappa + g_-^2 h^2}} - g_+ \right]. \end{aligned} \quad (7)$$

Thus, we have all the necessary expressions in explicit forms for the calculation of some important parameters of the magnetocaloric effect: the isentropes and the adiabatic cooling intensity $(\frac{\partial T}{\partial h})_S$, or the Grüneisen parameter

$$\Gamma_h = \frac{1}{T} \left(\frac{\partial T}{\partial h} \right)_S = -\frac{1}{c(T, h)} \frac{\partial m(T, h)}{\partial T}$$

(see, e.g., works [22, 27, 46, 47, 66–69]).

3. Results of Numerical Calculations

Let us now briefly dwell on the results of numerical calculations. Below, without loss of generality, we put $g_1 = 1$ and $J = 1$. We also confine the consideration to the g_2 -values $g_2 \in [-1, 1]$.

The magnetocaloric effect in a uniform system ($g_1 = g_2$) was studied in considerable details in work [22]. Here, the influence of the system non-uniformity will be analyzed first on the adiabatic change of the temperature with the change of the magnetic field, and then on the intensity of adiabatic cooling.

As was said above, if $g_2 > 0$, quantum phase transitions occur in the ground state at $h = h_s$. They manifest themselves in the magnetocaloric effect in the low-temperature interval (see Fig. 1). Namely, the isentropes have rather sharp slopes near the critical magnetic fields (there are clearly identified minima in the adiabatic dependence of the temperature on h). If $g_2 \leq 0$, the system is in the ground state and does not undergo any phase transition with the change of the magnetic field (the saturation is reached only at $h \rightarrow \infty$). Therefore, the isentropes at small S -values (see Fig. 2) have no aforementioned minima associated with quantum phase transitions (as it was in the case with positive g_2 -values).

Let us analyze in more details how the non-uniformity of the system affects the adiabatic change of the temperature, when the magnetic field varies. This influence is especially evident at low temperatures. In Figs. 1 and 2, the gradient maps of the entropy as a function of the magnetic field and the temperature are depicted for various values of the parameter g_2 . The plotted isentropes correspond to the following S -values: 0.01 and 0.03 (white curves); 0.05, 0.1, and 0.15 (light gray curves); 0.2, 0.3, and 0.4 (dark gray curves); and 0.5 and 0.6 (black curves). When “moving” along the isentrope, the temperature changes adiabatically with the change of the magnetic field. From Figs. 1 and 2, one can see the main aspect of the magnetocaloric effect change with the g_2 -factor change. Note that since the entropy is an even function of the magnetic field, the analysis can be confined to positive h -values. It is evident that the isentropes have extrema at $h = 0$.

Let us first consider the case $g_2 > 0$ (Fig. 1). If $g_2 = 1$, the isentropes plotted for small S -values ($S = 0.01 \div 0.3$) have one maximum at $h = 0$ and one minimum at a field h relatively close to h_s . The smaller the entropy, the closer the latter value to h_s .

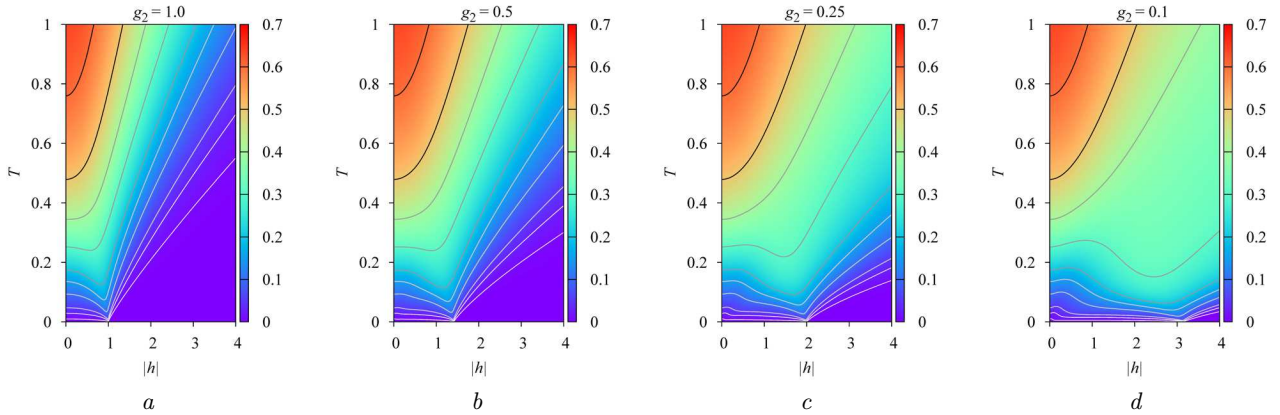


Fig. 1. Gradient maps of the entropy as a function of the magnetic field and the temperature at $g_2 = 1$ (a), 0.5 (b), 0.25 (c), and 0.1 (d). The isentrope curves correspond to $S = 0.01, 0.03$ (white curves), 0.05, 0.1, 0.15 (light gray curves), 0.2, 0.3, 0.4 (dark gray curves), and 0.5, 0.6 (black curves). Quantum phase transitions occur at $h_s = 1, 1.414, 2,$ and 3.162 for $g_2 = 1, 0.5, 0.25,$ and $0.1,$ respectively

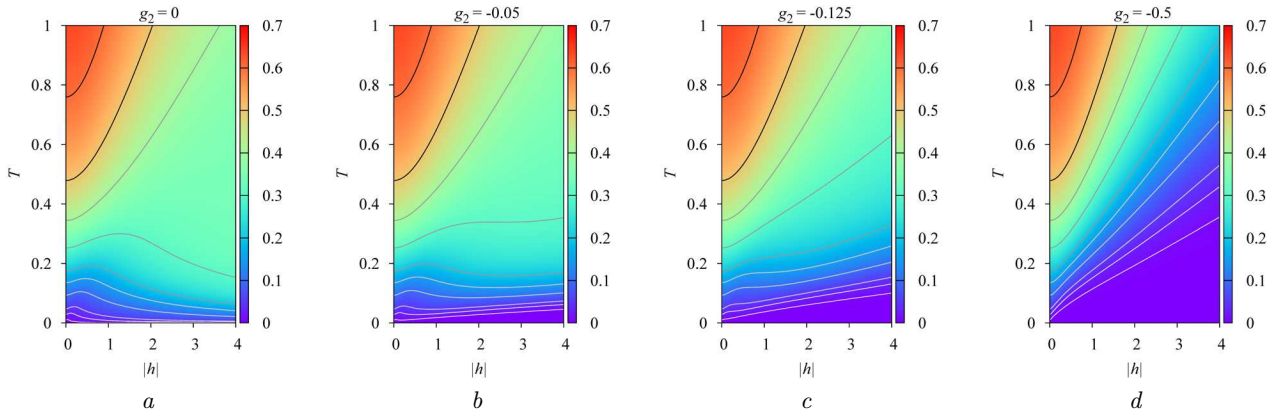


Fig. 2. Gradient maps of the entropy as a function of the magnetic field and the temperature at $g_2 = 0$ (a), -0.05 (b), -0.125 (c), and -0.5 (d). The isentrope curves correspond to $S = 0.01, 0.03$ (white curves), 0.05, 0.1, 0.15 (light gray curves), 0.2, 0.3, 0.4 (dark gray curves), and 0.5, 0.6 (black curves)

If $g_2 \in]0, 1[$, the isentropes corresponding to small S -values have a minimum at $h = 0$ (unlike the maximum in the uniform case) and a minimum at h close to h_s (similarly to the case $g_2 = 1$). In addition, there can be another minimum located between the mentioned ones. This additional isentrope minimum – and, accordingly, two maxima – appears only at sufficiently small S -values; and the smaller g_2 , the higher the entropy at which additional extrema takes place. For instance, one can see from Fig. 1 that if $g_2 = 0.5$ or 0.25 , only the curve for the constant entropy $S = 0.01$ has those three additional extrema, whereas, in the case $g_2 = 0.1$, those extrema are observed in the isoentropes plotted for $S = 0.01$ and 0.03 .

For some higher entropy values, the isentropes have only one maximum between the minimum at $h = 0$ and the minimum associated with the quantum phase transition (see the results for $S = 0.03 \div 0.15$ at $g_2 = 0.5$, for $S = 0.03 \div 0.3$ at $g_2 = 0.25$, and for $S = 0.05 \div 0.3$ at $g_2 = 0.1$). In other words, if, e.g., $g_2 = 0.25$ and $S = 0.01$, the following adiabatic processes run one by one as the magnitude of the magnetic field in the system increases: heating, drastic cooling, slow heating, cooling (its rate increases as $|h_s|$), and, finally, rather fast heating. For the same time $g_2 = 0.25$ but for $S = 0.03$, the observed sequence is as follows: heating, cooling (rather fast both at small $|h|$ and at $|h|$ close to $|h_s|$), and, finally, quick heating.

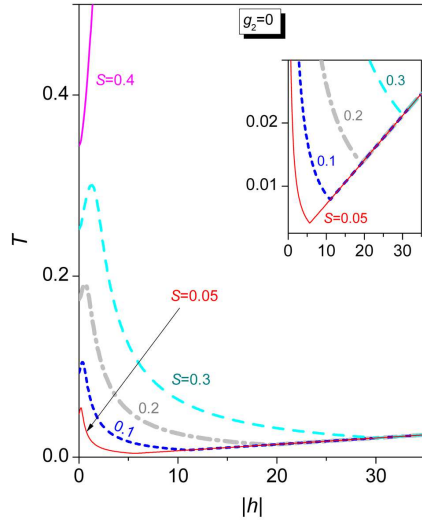


Fig. 3. Isoentropes plotted in the case $g_2 = 0$ for various entropy values $S = 0.05, 0.1, 0.2, 0.3,$ and 0.4

Now, let us consider the case $g_2 \leq 0$ (Fig. 2). If $g_2 = 0$ or -0.05 , the isentropes plotted for small S -values are nonmonotonic functions of the magnetic field: they have two minima (one of them at $h = 0$) and one maximum. If $g_2 = 0$, such behavior is observed for the isentropes corresponding to $S = 0.01 \div 0.3$ (see also Fig. 3). But if $g_2 = -0.05$, only the isentropes for $S = 0.01 \div 0.2$ have those three extrema, whereas the isentrope for $S = 0.3$ has only one minimum at $h = 0$. It is of interest that, in the case $g_2 = 0$, the minimum point at $h \neq 0$ on the isentropes is simultaneously a cusp. Furthermore, at $|h|$ larger than the cusp $|h|$ -value, the isentropes corresponding to different entropy values are superimposed (see Fig. 3).

If $g_2 = -0.125$ or -0.5 , the isentropes corresponding to small S -values have only one minimum at $h = 0$ (see Fig. 2). In the case $g_2 = -0.125$, the isentropes for $S = 0.01 \div 0.2$ demonstrate distinct inflection points at small h -values (a sort of “remnants” of the extrema at larger g_2 ; cf. the cases $g_2 = -0.05$ and -0.125). But there are no such inflection points, if $g_2 = -0.5$.

Let us now analyze how the field dependences of the adiabatic cooling intensity $(\frac{\partial T}{\partial h})_S$ (or the Grüneisen parameter Γ_h) change with the variation of g_2 and the temperature (see Figs. 4–6). Since $\Gamma_h(h)$ is an odd function of the magnetic field, we will confine our study to positive h -values.

It is known that, in systems with quantum phase transitions, if the temperature is low, $\Gamma_h(h)$ changes its sign at h that is close to the critical value h_s (see work [22] and references therein). It is clear that the lower T , the closer h to h_s . This can be seen from the presented figures for $g_2 = 1, 0.9, 0.5, 0.1,$ and 0.03 . At sufficiently high temperatures, $\Gamma_h(h)$ does not change its sign for both $g_2 > 0$ and $g_2 < 0$, and is positive over the whole interval $h \in]0, \infty[$.

Recall that, in the uniform case at low temperatures ($T = 0.01, 0.05,$ and 0.1), the Grüneisen parameter as a function of the magnetic field has one minimum and one maximum, but it has only one maximum at high temperatures ($T = 0.5$). Furthermore, if the temperature T is low and $h > 0$, the parameter $\Gamma_h(h)$ intersects the abscissa axis only once.

A small deviation from uniformity (the case $g_2 = -0.9$) leads to the appearance of additional extrema at low temperatures: three at $T = 0.001$ and 0.01 , and one at $T = 0.02$. Hence, the field dependence of the Grüneisen parameter has three maxima and two minima at $T = 0.001$ and 0.01 , and two maxima and one minimum at $T = 0.02$. Moreover, at $T = 0.001$ there are three additional points where $\Gamma_h(h)$ changes its sign. But, at the temperatures $T = 0.01$ and 0.02 , there is only one such additional point. It should be noted that those additional points, where $\Gamma_h(h) = 0$ (at smaller h 's) are not associated with any quantum phase transition. At the same time, it is the last change in the sign of the Grüneisen parameter with the increasing magnetic field (this is the fourth sign change for $T = 0.001$, and the second one for $T = 0.01$ and 0.02) at the h -values rather close to h_s that testifies to the phase transition in the ground state (similarly to other g_2 -values from the interval $]0, 1[$). At $T = 0.05$ and 0.1 , the dependences $\Gamma_h(h)$ have only two extrema each and change their sign in the interval $h \in]0, \infty[$ only once (similarly to the case $g_2 = 1$ at $T = 0.01, 0.05,$ and 0.1). It is clear that this sign change is also connected to the presence of the quantum phase transition.

The case $g_2 = 0.5$ is slightly more complicated than that considered above. There are three additional extrema at $T = 0.01$ and 0.05 , one at $T = 0.1$ and 0.27 , and none at the intermediate temperature $T = 0.2$ (i.e., at $T = 0.2$ the parameter $\Gamma_h(h)$ has only one minimum and one maximum, similarly to the cases $g_2 = 1$ at low temperatures and $g_2 = 0.9$ at $T = 0.05$

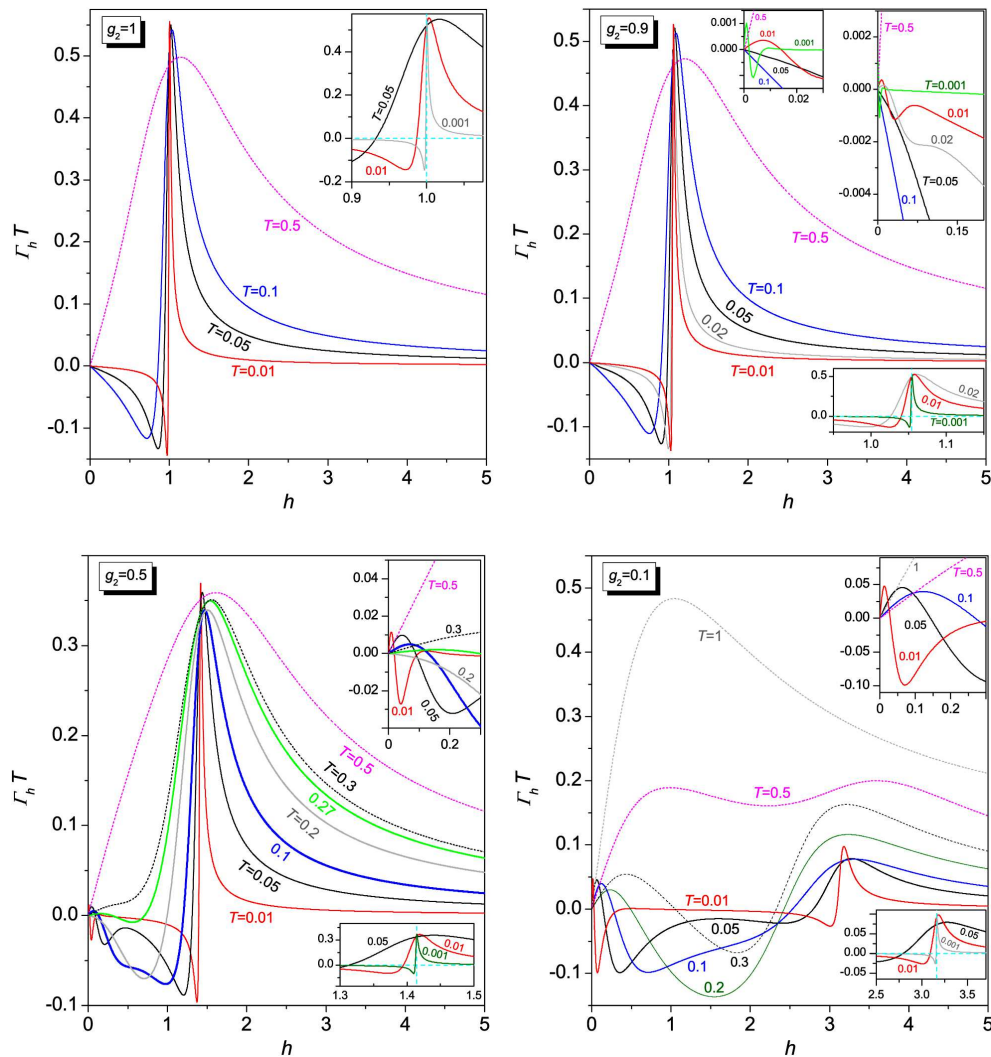


Fig. 4. Field dependences of the adiabatic cooling intensity $(\partial T/\partial h)_S = T\Gamma_h$ at $g_2 = 1, 0.9, 0.5,$ and $0.1,$ and various temperatures. Intersections of vertical and horizontal dashed lines in the insets correspond to the points where Γ_h changes its sign when T is close to zero, which is associated with quantum phase transitions ($h_s = 1, 1.054, 1.414$ and 3.162 for $g_2 = 1, 0.9, 0.5$ and $0.1,$ respectively)

and 0.1). Hence, one can see that the main difference between the cases $g_2 = 0.5$ and 0.9 consists in that the number of $\Gamma_h(h)$ extrema can only decrease as the temperature increases, if $g_2 = 0.9$, but it can also increase once (from two to three), if $g_2 = 0.5$.

Let us briefly dwell on the number of points, where the Grüneisen parameter changes its sign. At $g_2 = 0.5$ and $T = 0.01$, there are three additional points, where $\Gamma_h(h) = 0$ (together with the point close to h_s , their number equals four at $h > 0$). The dependence $\Gamma_h(h)$ intersects the abscissa axis at $h > 0$ twice at

the temperatures $T = 0.05, 0.1,$ and $0.27,$ and only once at $T = 0.2$.

As concerning the variation in the number of extrema in the field dependences of Γ_h with the temperature growth, the cases $g_2 = 0.1$ and 0.03 are somewhat similar to the case $g_2 = 0.9$. In particular, for $g_2 = 0.1$ at $T = 0.01$ and 0.05 , as well as for $g_2 = 0.03$ at $T = 0.01$, the Grüneisen parameter has three maxima and two minima (similarly as for $g_2 = 0.9, T = 0.01$). For $g_2 = 0.1$ at $T = 0.1, 0.2, 0.3,$ and $0.5,$ as well as for $g_2 = 0.03$

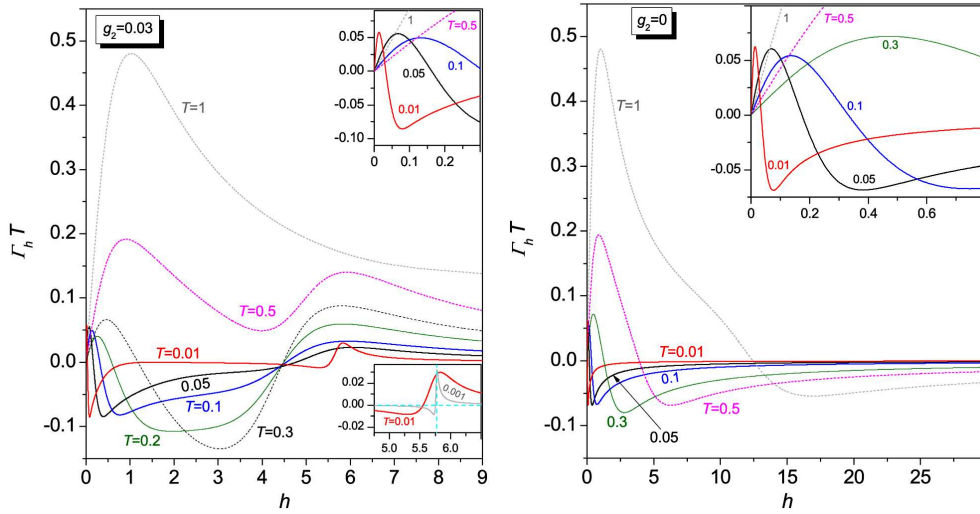


Fig. 5. Field dependences of the adiabatic cooling intensity $(\partial T/\partial h)_S = T\Gamma_h$ at $g_2 = 0.03$ and 0 , and various temperatures. Intersections of vertical and horizontal dashed lines in the lower inset in the left panel correspond to the point where Γ_h changes its sign when T is close to zero, which is associated with a quantum phase transition ($h_s = 5.773$ for $g_2 = 0.03$)

at $T = 0.05, 0.1, 0.2, 0.3$, and 0.5 , it has two maxima and one minimum (similarly as for $g_2 = 0.9$, $T = 0.02$). However, in contrast to the cases close to uniform ($g_2 = 0.9$) and nonuniform ones, in the considered cases with strong deviations from uniformity ($g_2 = 0.1$ and 0.03), there is no temperature at which $\Gamma_h(h)$ would have one minimum and one maximum at positive fields. Thus, a “transition” from a $\Gamma_h(h)$ -curve with several extrema to a curve with one maximum occurs at $g_2 = 0.1$ and 0.03 differently than at $g_2 = 1$ and 0.9 . In the cases with strong deviations from uniformity, the second and third extrema (at higher h 's), so to speak, “merge” and disappear, as the temperature increases. On the other hand, in the uniform case and the case with weak deviations from uniformity, the first extremum becomes less pronounced, as the temperature T grows, then approaches the coordinate origin, and finally disappears. A brief description of the temperature behavior of the first two extrema (the maximum and the minimum at small h 's) in the field dependences of the adiabatic cooling intensity will be made later, when we will analyze the case $g_2 = 0$.

As concerning the variation in the number of points, where $\Gamma_h(h) = 0$, from Fig. 4 and the left panel in Fig. 5, one can see that, in the cases $g_2 = 0.1$ and 0.03 , the situations are somewhat different; at the same time, they are somewhat similar to and

somewhat different from the situations for the cases $g_2 = 0.9$ and 0.5 . For instance, for $g_2 = 0.1$ and 0.03 at $T = 0.01$, the parameter $\Gamma_h(h)$ with five extrema changes its sign four times at $h > 0$ (as it is for $g_2 = 0.9$ at $T = 0.001$ and for $g_2 = 0.5$ at $T = 0.01$). For $g_2 = 0.1$ at $T = 0.05$ and for $g_2 = 0.03$ at $T = 0.02$, $\Gamma_h(h)$, also with five extrema, crosses the abscissa axis in the interval $h \in]0, \infty[$ only two times (similarly as for $g_2 = 0.9$ at $T = 0.01$ and for $g_2 = 0.5$ at $T = 0.05$). For $g_2 = 0.1$ at $T = 0.1, 0.2$, and 0.3 , as well as for $g_2 = 0.03$ at $T = 0.05, 0.1, 0.2$, and 0.3 , the Grüneisen parameter, with three extrema, changes its sign twice (as it is for $g_2 = 0.9$ at $T = 0.02$ and for $g_2 = 0.5$ at $T = 0.1$ and 0.27). At the same time, in the cases $g_2 = 0.1$ and 0.03 at $T = 0.5$, $\Gamma_h(h)$ is a non-monotonic function with three extrema, which is positive over the whole interval $h > 0$ (the Grüneisen parameter does not demonstrate a similar behavior, if $g_2 = 0.9$ or 0.5). On the other hand, in the cases with strong deviations from uniformity ($g_2 = 0.1$ and 0.03), there is no temperature at which $\Gamma_h(h)$ changes its sign once at $h > 0$, although such behavior can be observed at certain T 's for $g_2 = 1, 0.9$, and 0.5 . Finally, at low temperatures ($T = 0.01$), the last two extrema (there is a point between them where $\Gamma_h(h) = 0$ and which is associated with the quantum phase transition) at $g_2 = 0.03$ are much less “pronounced” than the first two, which

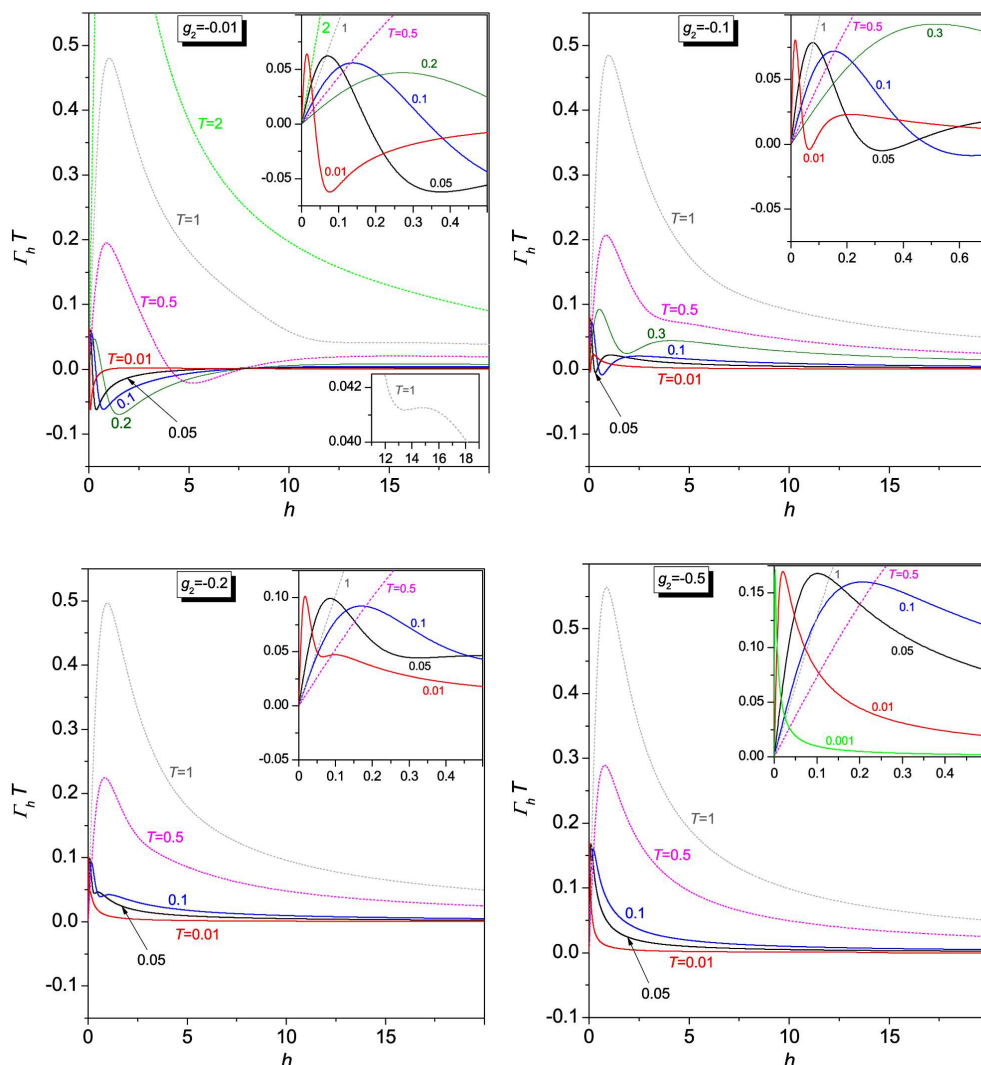


Fig. 6. Field dependences of the adiabatic cooling intensity $(\partial T/\partial h)_S = T\Gamma_h$ at $g_2 = -0.01, -0.1, -0.2,$ and -0.5 , and various temperatures

cannot be said about the case $g_2 = 0.1$. For $g_2 = 0.9$ and 0.5 at $T = 0.01$, those two last extrema are much more “pronounced” than the first two.

Let us briefly summarize the results obtained for the adiabatic cooling intensity $(\frac{\partial T}{\partial h})_S$, or the associated Grüneisen parameter Γ_h , in the case $g_2 > 0$ (Fig. 4 and the left panel in Fig. 5), when a quantum phase transition occurs in the system at $T \rightarrow 0$ [13]. From the above analysis, one can see that the temperature-induced changes in the behavior of either of the above-mentioned characteristics considered as functions of the magnetic field are different in different cases: uniform, close to uniform, the case of

small positive g_2 , and the intermediate case between the last two (an intermediate case between strong and weak deviations from uniformity). However, it should be noted that the situation is unambiguous at very high fields: the both functions are decreasing at any positive g_2 and finite temperatures, and tend to zero at $h \rightarrow \infty$.

Now, let us consider how the field dependences of the adiabatic cooling intensity (or the Grüneisen parameter) change with the changes of g_2 and the temperature in the case $g_2 \leq 0$ (see the right panel in Fig. 5 and Fig. 6). Since there are no phase transitions in the ground state with the change of the magnetic

field for such g_2 -values, it is natural that there is no corresponding point, where the sign of $\Gamma_h(h)$ would change and which would be related with a quantum phase transition (as it was in the case $g_2 > 0$). At the same time, if $g_2 \leq 0$, also absent are the corresponding extrema (the minimum and the maximum) between which there was the above-mentioned point $\Gamma_h(h) = 0$ (at fields close to h_s and low temperatures) in the case $g_2 > 0$.

First, let us analyze the results obtained for $g_2 = 0$, which are different from the results obtained for $g_2 \geq 0$. In the case $g_2 = 0$, the Grüneisen parameter has one maximum and one minimum at finite temperatures and crosses the abscissa axis once at $h > 0$. That is, $\Gamma_h(h)$ is an increasing function at large fields for any finite T (in contrast to the case $g_2 \neq 0$), and $\lim_{h \rightarrow \infty} \Gamma_h(h) = 0$. It should also be noted that, as the temperature increases, the maximum value in the field dependence of the adiabatic cooling intensity shifts toward higher h 's. If the temperature grows, but remains low, this maximum decreases insignificantly, but at high T , it increases rather drastically. A similar situation is also observed for the first maxima of $(\partial T / \partial h)_S = T \Gamma_h(h)$ if the g_2 -values are negative or small positive. At high T , the minimum value in the field dependence of the adiabatic cooling intensity changes relatively weakly, as the temperature increases, but its shift toward higher fields occurs faster than that of the maxima. Moreover, if the temperature is sufficiently low or high and grows, the absolute value of the minimum of $(\partial T / \partial h)_S = T \Gamma_h(h)$ decreases, but in the case of intermediate temperatures, it increases. Somewhat similar behavior is also demonstrated by the first minima in the cases of small g_2 -values [both positive ($g_2 = 0.1, 0.03$) and negative ($g_2 = -0.01$): as the temperature increases, the first minimum $(\partial T / \partial h)_S = T \Gamma_h(h)$ first slightly "grows", then "falls", and finally starts to "grow" again. For example, at $g_2 = 0.1$, the first minimum for $T = 0.1$ is higher than those for $T = 0.01$ and 0.2 , but lower than that for $T = 0.3$.

In the cases $g_2 = -0.01$ and -0.1 , and at not very high temperatures, the Grüneisen parameter has three extrema. At low T , it crosses the abscissa axis at $h > 0$ twice, but at higher T -values, it does not change its sign. Thus, $\Gamma_h(h)$ at $T = 1$ for $g_2 = -0.01$ and at $T = 0.3$ for $g_2 = -0.1$ has three extrema and is positive within the whole interval $h \in]0, \infty[$. But, for example, at $T = 0.5$ for $g_2 = -0.01$ or at $T = 0.3$ for

$g_2 = -0.1$, the Grüneisen parameter changes its sign two times. At sufficiently high temperatures ($T = 2$ for $g_2 = -0.01$, and $T = 0.5$ for $g_2 = -0.1$), $\Gamma_h(h)$ has only one extremum, similarly as it is at high T in the case of positive g_2 . By comparing the results obtained for $g_2 = -0.01$ and -0.1 , one can see that at $g_2 = -0.1$ at low temperatures (for example, $T = 0.01$ or 0.1), the absolute value of the minimum $\Gamma_h(h)$ is much smaller than the value of the first maximum, which cannot be said in the case $g_2 = -0.01$.

If $g_2 = -0.2$, the number of extrema in the field dependences of Γ_h changes with the increasing temperature in the same way as in the cases $g_2 = -0.01$ and -0.1 . That is, the Grüneisen parameter has three extrema at low temperatures, and one at high temperatures. At the same time, in the case $g_2 = -0.2$, unlike the cases $g_2 = -0.01$ and -0.1 considered above, $\Gamma_h(h)$ does not change its sign at $h > 0$ even at rather low temperatures.

Finally, let us consider the results obtained for $g_2 = -0.5$ (see Fig. 6). In this case, the Grüneisen parameter as a function of the magnetic field has only one maximum even at low temperatures and is positive within the whole interval $h > 0$. The same behavior of $\Gamma_h(h)$ takes place, if the deviation from uniformity is maximum ($g_2 = -1$).

Let us briefly summarize the results obtained for the adiabatic cooling intensity $(\frac{\partial T}{\partial h})_S$, or the related Grüneisen parameter Γ_h , in the case $g_2 \leq 0$ (right panel in Fig. 5 and Fig. 6), when the system in the ground state and under any magnetic fields is in the phase, where the Fermi level lies between two spectral branches [13]. The analysis of how the number of extrema in and the number of intersections of the abscissa axis by the field dependence of either of the above-mentioned characteristics change with the temperature showed that the case $g_2 = 0$, the case of small or large g_2 -values, and the intermediate case between them are different. Furthermore, only if $g_2 = 0$, the adiabatic cooling intensity and, accordingly, the Grüneisen parameter, are negative at strong positive magnetic fields.

4. Conclusions

The magnetocaloric effect in the one-dimensional spin- $\frac{1}{2}$ XX model with the periodically varying g -factors (g_1 and g_2) has been studied. In the case where g_1 and g_2 are of the same sign, the variation

of the magnetic field h induces the quantum phase transitions in the ground state between the phases with saturated magnetization and the gapless spin liquid, which manifests itself in the magnetocaloric effect. In particular, near the critical magnetic fields h_s , the isentropes corresponding to small values of the entropy S have minima, and the Grüneisen parameter $\Gamma_h(h)$ calculated for low temperatures changes its sign. Note that, for a better understanding, the following conclusions concern the field interval $h \geq 0$ (since the entropy is an even function of h , and $\Gamma_h(h)$ is an odd one). It should also be said that, when analyzing the isentropes and the Grüneisen parameter, we confined the consideration to the entropy values $S > 0.001$ and the temperature values $T > 0.001$, respectively.

- It is found that if $g_1 g_2 > 0$, and if the system is non-uniform ($g_1 \neq g_2$), there appear additional extrema in the isentropes plotted for small S -values: three extrema, if the entropy values are rather small, or one extremum for somewhat larger S -values. Furthermore, in the non-uniform case, the curves corresponding to a constant entropy have a minimum at $h = 0$, whereas they have maxima at $h = 0$ for small S -values in the uniform case.

- If either of two g -factors equals zero or if g_1 and g_2 have different signs, and if their absolute values are different by not less than about an order of magnitude, the isentropes corresponding to small entropy values have, besides the minimum at $h = 0$, two more extrema at $h > 0$. In the case $g_1 g_2 < 0$, those two extrema are more pronounced at not very small S -values and have, so to speak, the same origin as the first two additional extrema have (at $0 < h \ll h_s$) in the case where g_1 and g_2 are of the same sign and differ by values.

- It is shown that, at low temperatures, the deviation from the uniformity of g -factors (nevertheless, they remain to be of the same sign) leads to the appearance of three additional values of the magnetic field at which the Grüneisen parameter $\Gamma_h(h)$ crosses the abscissa axis and, accordingly, to the appearance of three additional extrema in the field dependence of this parameter (it is known that $\Gamma_h(h)$ has only two extrema at low T in the uniform case and is equal to zero only at $h = 0$ and at h close to h_s). It is important to note that, in the case of substantial non-uniformity of g -factors, the extrema of $\Gamma_h(h)$ near those two additional field values, where $\Gamma_h(h)$ changes

its sign, are much more pronounced than near h_s . In addition, it should be noted that the variation in the behavior of the field dependence of the Grüneisen parameter with the temperature occurs differently for different values of the ratio g_2/g_1 .

- When either of g -factors equals zero, the Grüneisen parameter as a function of the magnetic field has two extrema at any T and crosses the abscissa axis at $h \geq 0$ twice (for the first time, at $h = 0$). It should be noted that, only in this case, the parameter $\Gamma_h(h)$ is an increasing function of h at very high magnetic fields irrespective of the temperature. If the both g -factors differ from zero, Γ_h decreases with the increasing field (at large h and any T).

- In the case $g_1 g_2 < 0$, the dependence $\Gamma_h(h)$ has three extrema at low temperatures and crosses the abscissa axis three times (in the interval $h \in [0, \infty)$, only if the absolute values of g_1 and g_2 are different by not less than about an order of magnitude. As the difference between $|g_1|$ and $|g_2|$ decreases, the Grüneisen parameter (at low T) first preserves the three extrema mentioned above, but it is already positive within the whole interval $h \geq 0$ ($\Gamma_h(h) = 0$ only at $h = 0$). A further reduction of the difference between the absolute values of the g -factors preserves only one maximum in the field dependence of Γ_h .

- At low temperatures and small positive values of the magnetic field, $\Gamma_h(h)$ is an increasing function in the case $g_1 \neq g_2$ (irrespective of whether the g -factors are of the same or different signs), and a descending function in the case $g_1 = g_2$.

The author expresses gratitude to T.M. Verkholyak for his interest in this work, his help, advice, and useful discussion.

1. P. Bhatt, N. Thakur, M.D. Mukadam, S.S. Meena, S.M. Yusuf. One-dimensional single-chain molecular magnet with a cross-linked II-II coordination network $\{[\text{Co}^{\text{II}}(\Delta)\text{Co}^{\text{II}}(\Lambda)](\text{ox})_2(\text{phen})_2\}_n$. *J. Phys. Chem. C* **118**, 1864 (2014).
2. E. Coronado, M. Drillon, A. Fuertes, D. Beltran, A. Mosset, J. Galy. Structural and magnetic study of $\text{Ni}_2(\text{EDTA})(\text{H}_2\text{O})_4 \cdot 2\text{H}_2\text{O}$. Alternating Landé factors in a two-sublattice 1D system. *J. Am. Chem. Soc.* **108**, 900 (1986).
3. W.-G. Yin, X. Liu, A.M. Tselik, M.P.M. Dean, M.H. Upton, J. Kim, D. Casa, A. Said, T. Gog, T.F. Qi, G. Cao, J.P. Hill. Ferromagnetic exchange anisotropy from antiferromagnetic superexchange in the mixed $3d-5d$ transition-

- metal compound $\text{Sr}_3\text{CuIrO}_6$. *Phys. Rev. Lett.* **111**, 057202 (2013).
4. W.-G. Yin, C.R. Roth, A.M. Tsvelik. *Spin Frustration and a "Half Fire, Half Ice" Critical Point from Nonuniform g -Factors*. [https://arxiv.org/abs/1510.00030].
 5. F. Souza, M.L. Lyra, J. Strečka, M.S.S. Pereira. Magnetization processes and quantum entanglement in a spin- $\frac{1}{2}$ Ising–Heisenberg chain model of a heterotrimetallic Fe–Mn–Cu coordination polymer. *J. Magn. Magn. Mater.* **471**, 423 (2019).
 6. W. Van den Heuvel, L.F. Chibotaru. Dysprosium-based experimental representatives of an Ising–Heisenberg chain and a decorated Ising ring. *Phys. Rev. B* **82**, 174436 (2010).
 7. M. Oshikawa, I. Affleck. Field-induced gap in $S=1/2$ antiferromagnetic chains. *Phys. Rev. Lett.* **79**, 2883 (1997).
 8. I. Affleck, M. Oshikawa. Field-induced gap in Cu benzoate and other $S = \frac{1}{2}$ antiferromagnetic chains. *Phys. Rev. B* **60**, 1038 (1999).
 9. M. Kenzelmann, C. D. Batista, Y. Chen, C. Broholm, D.H. Reich, S. Park, Y. Qiu. $S = \frac{1}{2}$ chain in a staggered field: High-energy bound-spinon state and the effects of a discrete lattice. *Phys. Rev. B* **71**, 094411 (2005).
 10. O. Derzhko. Jordan–Wigner fermionization for spin- $\frac{1}{2}$ systems in two dimensions: A brief review. *J. Phys. Stud.* **5**, 49 (2001).
 11. E. Lieb, T. Schultz, D. Mattis. Two soluble models of an antiferromagnetic chain. *Ann. Phys. (N.Y.)* **16**, 407 (1961).
 12. V.M. Kontorovich, V.M. Tsukernik. Magnetic properties of a spin array with two sublattices. *Sov. Phys. JETP* **26**, 687 (1968).
 13. T. Krokhnalskii, T. Verkholyak, O. Baran, V. Ohanyan, O. Derzhko. Spin- $\frac{1}{2}$ XX chain in a transverse field with regularly alternating g factors: Static and dynamic properties. *Phys. Rev. B* **102**, 144403 (2020).
 14. O. Derzhko, T. Krokhnalskii. Dynamic structure factor of the spin- $\frac{1}{2}$ transverse Ising chain. *Phys. Rev. B* **56**, 11659 (1997).
 15. O. Derzhko, T. Krokhnalskii, J. Stolze. Dynamics of the spin- $\frac{1}{2}$ isotropic XY chain in a transverse field. *J. Phys. A* **33**, 3063 (2000).
 16. J.P. de Lima, L.L. Gonçalves, T.F.A. Alves. Anisotropic XY model on the inuniform periodic chain. *Phys. Rev. B* **75**, 214406 (2007).
 17. T. Antal, Z. Rácz, A. Rákos, G.M. Schütz. Isotropic transverse XY chain with energy and magnetization currents. *Phys. Rev. E* **57**, 5184 (1998).
 18. I. Titvinidze, G. Japaridze. Phase diagram of the spin $S = 1/2$ extended XY model. *Eur. Phys. J. B* **32**, 383 (2003).
 19. A.A. Zvyagin. Quantum phase transitions in low-dimensional quantum spin systems with incommensurate magnetic structures. *Phys. Rev. B* **72**, 064419 (2005).
 20. P. Lou. Quantum phase transition in a solvable spin model. *Phys. Rev. B* **72**, 064435 (2005).
 21. T. Krokhnalskii, O. Derzhko, J. Stolze, T. Verkholyak. Dynamic properties of the spin- $\frac{1}{2}$ XY chain with three-site interactions. *Phys. Rev. B* **77**, 174404 (2008).
 22. M. Topilko, T. Krokhnalskii, O. Derzhko, V. Ohanyan. Magnetocaloric effect in spin- $\frac{1}{2}$ XX chains with three-spin interactions. *Eur. Phys. J. B* **85**, 278 (2012).
 23. O. Menchyshyn, V. Ohanyan, T. Verkholyak, T. Krokhnalskii, O. Derzhko. Magnetism-driven ferroelectricity in spin- $\frac{1}{2}$ XY chains. *Phys. Rev. B* **92**, 184427 (2015).
 24. O.R. Baran. Energy flux effect in the one-dimensional spin- $\frac{1}{2}$ XX model of magnetoelectric. Lagrange multiplier method. *Ukr. J. Phys.* **66**, 890 (2021).
 25. H. Katsura, N. Nagaosa, A.V. Balatsky. Spin current and magnetoelectric effect in noncollinear magnets. *Phys. Rev. Lett.* **95**, 057205 (2005).
 26. M. Brockmann, A. Klümper, V. Ohanyan. Exact description of magnetoelectric effect in the spin- $\frac{1}{2}$ XXZ chain with Dzyaloshinskii–Moriya interaction. *Phys. Rev. B* **87**, 054407 (2013).
 27. O. Baran, V. Ohanyan, T. Verkholyak. Spin- $\frac{1}{2}$ XY chain magnetoelectric: Effect of zigzag geometry. *Phys. Rev. B* **98**, 064415 (2018).
 28. V. Ohanyan. Influence of XY anisotropy on a magnetoelectric effect in spin- $\frac{1}{2}$ XY chain in a transverse magnetic field. *Condens. Matter Phys.* **23**, 43704 (2020).
 29. V. Eisler, Z. Rácz, F. van Wijland. Magnetization distribution in the transverse Ising chain with energy flux. *Phys. Rev. E* **67**, 056129 (2003).
 30. J. Li, S. Lei. Thermodynamic properties of the spin- $\frac{1}{2}$ ferromagnetic Heisenberg chain with long-range interactions. *Phys. Lett. A* **372**, 4086 (2008).
 31. J.-S. Caux, F.H.L. Essler, U. Löw. Dynamical structure factor of the anisotropic Heisenberg chain in a transverse field. *Phys. Rev. B* **68**, 134431 (2003).
 32. R. Hagemans, J.-S. Caux, U. Löw. Gapped anisotropic spin chains in a field. *Phys. Rev. B* **71**, 014437 (2005).
 33. H.H. Fu, K.L. Yao, Z.L. Liu. Thermodynamic properties of a spin- $\frac{1}{2}$ diamond chain as a model for a molecule-based ferrimagnet and the compound $\text{Cu}_3(\text{CO}_3)_2(\text{OH})_2$. *Phys. Rev. B* **73**, 104454 (2006).
 34. T. Verkholyak, J. Strečka, M. Jaščur, J. Richter. Magnetic properties of the quantum spin- $\frac{1}{2}$ XX diamond chain: the Jordan–Wigner approach. *Eur. Phys. J. B* **80**, 433 (2011).
 35. Y.R. Wang. Ground state of the two-dimensional antiferromagnetic Heisenberg model studied using an extended Wigner–Jordan transformation. *Phys. Rev. B* **43**, 3786 (1991).
 36. E. Fradkin. Jordan–Wigner transformation for quantum-spin systems in two dimensions and fractional statistics. *Phys. Rev. Lett.* **63**, 322 (1989).
 37. A. Lopez, A.G. Rojo, E. Fradkin. Chern–Simons theory of the anisotropic quantum Heisenberg antiferromagnet on a square lattice. *Phys. Rev. B* **49**, 15139 (1994).
 38. O. Derzhko, T. Verkholyak, R. Schmidt, J. Richter. Square-lattice $s = 1/2$ XY model and the Jordan–Wigner

- fermions: The ground-state and thermodynamic properties. *Physica A* **320**, 407 (2003).
39. O. Derzhko, T. Krokhmalksii. Dynamics of zz spin correlations in the square-lattice spin- $\frac{1}{2}$ isotropic XY model. *Physica B* **337**, 357 (2003).
 40. O. Derzhko, T. Krokhmalksii. Jordan–Wigner approach to dynamic correlations in 2D spin- $\frac{1}{2}$ models. *Czech. J. Phys.* **55**, 601 (2005).
 41. O.R. Baran, T. M. Verholyak. Ground state of two-dimensional spin- $\frac{1}{2}$ $J_1 - J_2$ Heisenberg models in the Jordan–Wigner fermionization approach. *J. Phys. Stud.* **19**, 4701 (2015).
 42. O.R. Baran, T.M. Verkholyak. Two-dimensional spin- $\frac{1}{2}$ $J_1 - J'_1 - J_2$ Heisenberg model within Jordan–Wigner transformation. *Ukr. J. Phys.* **61**, 597 (2016).
 43. T. Jolicœur, G. Misguich, S.M. Girvin. Magnetization process from Chern–Simons theory and its application to $\text{SrCu}_2(\text{BO}_3)_2$. *Progr. Theor. Phys. Suppl.* **145**, 76 (2002).
 44. D. Eliezer, G. Semenoff. Anyonization of lattice Chern–Simons theory. *Ann. Phys.* **217**, 66 (1992).
 45. L. Čanová, J. Strečka, T. Lučivjanský. Exact solution of the mixed spin- $\frac{1}{2}$ and spin- S Ising–Heisenberg diamond chain. *Condens. Matter Phys.* **12**, 353 (2009).
 46. C. Trippe, A. Honecker, A. Klümper, V. Ohanyan. Exact calculation of the magnetocaloric effect in the spin- $\frac{1}{2}$ XXZ chain. *Phys. Rev. B* **81**, 054402 (2010).
 47. B. Wolf, A. Honecker, W. Hofstetter, U. Tutsch, M. Lang. Cooling through quantum criticality and many-body effects in condensed matter and cold gases. *Int. J. Mod. Phys. B* **28**, 1430017 (2014).
 48. E. Warburg. Magnetische Untersuchungen. *Ann. Phys. (Leipzig)* **13**, 141 (1881).
 49. W.F. Giaque, D.P. MacDougall. Attainment of temperatures below 1° absolute by demagnetization of $\text{Gd}_2(\text{SO}_4)_3 \cdot 8\text{H}_2\text{O}$. *Phys. Rev.* **43**, 768 (1933).
 50. A.S. Oja, O.V. Lounasmaa. Nuclear magnetic ordering in simple metals at positive and negative nanokelvin temperatures. *Rev. Mod. Phys.* **69**, 1 (1997).
 51. P. Strehlow, H. Nuzha, E. Bork. Construction of a nuclear cooling stage. *J. Low. Temp. Phys.* **147**, 81 (2007).
 52. A.A. Zvyagin. Magnetic ordering of anisotropic magnets due to rotation of the magnetic field. *Low Temp. Phys.* **43**, 1194 (2017).
 53. K.A. Gschneidner Jr., V.K. Pecharsky, A.O. Tsokol. Recent developments in magnetocaloric materials. *Rep. Prog. Phys.* **68**, 1479 (2005).
 54. A.M. Tishin, Y.I. Spichkin. *The Magnetocaloric Effect and its Applications* (Institute of Physics, 2003).
 55. S. Sachdev. *Quantum Phase Transitions* (Cambridge University Press, 2011).
 56. B. Wolf, Y.K. Tsui, D. Jaiswal-Nagar, U. Tutsch, A. Honecker, K. Remović-Langer, G. Hofmann, A. Prokofiev, W. Assmus, G. Donath, M. Lang. Magnetocaloric effect and magnetic cooling near a field-induced quantum-critical point. *Proc. Natl. Acad. Sci. USA* **108**, 6862 (2011).
 57. M.E. Zhitomirsky, A. Honecker. Magnetocaloric effect in one-dimensional antiferromagnets. *J. Stat. Mech.: Theor. Exp.* **2004**, P07012 (2004).
 58. J. Strečka, O. Rojas, T. Verkholyak, M.L. Lyra. Magnetization process, bipartite entanglement, and enhanced magnetocaloric effect of the exactly solved spin- $\frac{1}{2}$ Ising–Heisenberg tetrahedral chain. *Phys. Rev. E* **89**, 022143 (2014).
 59. L. Gálisová, J. Strečka. Magnetic Grüneisen parameter and magnetocaloric properties of a coupled spin–electron double-tetrahedral chain. *Phys. Lett. A* **379**, 2474 (2015).
 60. L. Gálisová, J. Strečka. Vigorous thermal excitations in a double-tetrahedral chain of localized Ising spins and mobile electrons mimic a temperature-driven first-order phase transition. *Phys. Rev. E* **91**, 022134 (2015).
 61. L. Gálisová. Magnetocaloric effect in the symmetric spin- $\frac{1}{2}$ diamond chain with different Landé g -factors of the Ising and Heisenberg spins. *Acta Mech. Slovaca.* **19**, 46 (2015).
 62. H.A. Zad, N. Ananikian, M. Jaščur. Single-ion anisotropy effects on the demagnetization process of the alternating weak-rung interacting mixed spin-(1/2, 1) Ising–Heisenberg double saw-tooth ladders. *Phys. Scripta* **95**, 095702 (2020).
 63. L. Gálisová. Reentrant phenomenon and inverse magnetocaloric effect in a generalized spin-(1/2, s) Fisher’s superexchange antiferromagnet. *J. Phys.: Condens. Matter* **28**, 476005 (2016).
 64. L. Gálisová, J. Strečka. Magnetic and magnetocaloric properties of the exactly solvable mixed-spin Ising model on a decorated triangular lattice in a magnetic field. *Physica E* **99**, 244 (2018).
 65. J. Strečka, K. Karl’ová. Weak singularities of the isothermal entropy change as the smoking gun evidence of phase transitions of mixed-spin Ising model on a decorated square lattice in transverse field. *Entropy* **23**, 1533 (2021).
 66. L. Zhu, M. Garst, A. Rosch, Q. Si. Universally diverging Grüneisen parameter and the magnetocaloric effect close to quantum critical points. *Phys. Rev. Lett.* **91**, 066404 (2003).
 67. M. Garst, A. Rosch. Sign change of the Grüneisen parameter and magnetocaloric effect near quantum critical points. *Phys. Rev. B* **72**, 205129 (2005).
 68. T. Zajarniuk, A. Szewczyk, P. Wiśniewski, M.U. Gutowska, R. Puzniak, H. Szymczak, I. Gudim, V.A. Bedarev, M.I. Pashchenko, P. Tomczak, W. Szuszkiewicz. Quantum versus classical nature of the low-temperature magnetic phase transition in $\text{TbAl}_3(\text{BO}_3)_4$. *Phys. Rev. B* **105**, 094418 (2022).
 69. A.P. Moina. Negative/positive electrocaloric effect in antiferroelectric squaric acid. *J. Appl. Phys.* **133**, 094101 (2023).

Received 26.04.23.

Translated from Ukrainian by O.I. Voitenko

O.P. Baran

МАГНЕТОКАЛОРИЧНИЙ ЕФЕКТ
У СПІН-1/2 ОДНОВИМІРНІЙ ХХ МОДЕЛІ
З ДВОМА РЕГУЛЯРНОЗМІННИМИ g -ФАКТОРАМИ

Досліджено вплив неоднорідності g -факторів, коли вони є регулярнозмінними з періодом два, на магнетокалоричний ефект у спін-1/2 ХХ ланцюжку в поперечному магнітному полі. За допомогою перетворення Йордана–Вігнера задача зводиться до гамільтоніана невзаємодіючих безспінових ферміонів і розв'язується точно. Проаналізовано, як зміню-

ються ізоентропи та польові залежності параметра Грюнайзена зі зміною g_2/g_1 . Основна увага приділяється низькотемпературній області. Показано відмінності магнетокалоричного ефекту у випадках, коли g -фактори мають однакові та різні знаки, а також коли один із g -факторів дорівнює нулю.

Ключові слова: одновимірні квантові спінові моделі, g -фактор, ферміонізація Йордана–Вігнера, магнетокалоричний ефект, квантовий фазовий перехід.